



Investigation on Rod Bundle CHF Mechanistic Model for DNB and DO Prediction Under Wide Parameter Range

Wei Liu*, Shinian Peng, Guangming Jiang and Yu Liu

State Key Laboratory of Reactor System Design Technology, Nuclear Power Institute of China, Chengdu, China

OPEN ACCESS

Edited by:

Jinbiao Xiong,
Shanghai Jiao Tong University, China

Reviewed by:

Liangming Pan,
Chongqing University, China
Ivo Kljenak,
Institut Jožef Stefan (IJS), Slovenia

*Correspondence:

Wei Liu
liuwei0958@126.com

Specialty section:

This article was submitted to
Nuclear Energy,
a section of the journal
Frontiers in Energy Research

Received: 24 October 2020

Accepted: 23 April 2021

Published: 13 May 2021

Citation:

Liu W, Peng S, Jiang G and Liu Y
(2021) Investigation on Rod Bundle
CHF Mechanistic Model for DNB and
DO Prediction Under Wide
Parameter Range.
Front. Energy Res. 9:620970.
doi: 10.3389/fenrg.2021.620970

For a water cooled reactor, the key thermal-hydraulic parameters span a wide range corresponding to different CHF regimes. Under accident conditions, due to the flow regime transition and interchannel mixing effect, the corresponding CHF can transition from the DO to DNB regime. In order to continuously and accurately predict DNB and DO regime CHF under wide parameter range for rod bundle channel, a comprehensive CHF mechanistic model covering the DNB and DO regime CHF prediction is established based on the rod bundle CHF-regime criterion. The DNB regime CHF mechanistic model of superheated liquid layer depletion under turbulence fluctuation bubbles and the mature DO regime CHF mechanistic model are combined to form the comprehensive CHF model. Furthermore, the comprehensive CHF model is assessed by 5 × 5 rod bundle CHF experimental data independently obtained by the Nuclear Power Institute of China (NPIC). The statistical evaluation and parametric trend analysis show that the maximum mean error of P/M is within ±22%, and the local pressure, mass flux, and quality do not have any effects on the average deviations of the predicted flux P from the measured flux M. This indicates that the comprehensive CHF mechanistic model can accurately and continuously predict the DNB and DO regime CHF in the rod bundle channel.

Keywords: departure from nucleate boiling, dryout, rod bundle channel, critical heat flux, mechanistic model

INTRODUCTION

Critical heat flux (CHF) is an important thermal safety limit in the research and development of nuclear fuel assemblies and reactor thermal-hydraulic design and safety analysis. According to the different flow regimes and heat transfer characteristics corresponding to CHF, the flow boiling crisis in rod bundle channel can be divided into DNB regime and dryout (DO) regime (Tong, 1967).

For the pressurized water reactor (PWR), subcooled nucleate boiling occurs at the hot channel exit under normal operation conditions. Thus, the DNB regime CHF is the most likely to occur due to the low vapor quality in the channel. Under accident conditions, there are several kinds of flow regimes existing in the rod bundle channel. Moreover, due to the interchannel mixing mechanisms (Xiong et al., 2020) and the cross flow caused by the mixing vanes between adjacent open channels (Qu et al., 2019), the flow regime

Abbreviations: CHF, critical heat flux; DNB, departure from nucleate boiling; DO, dryout; HP, high pressure; NPIC, Nuclear Power Institute of China; PWR, pressurized water reactor.

could transition from annular flow to bubble flow or slug flow. Accordingly, the corresponding CHF will also transition from the DO to DNB regime (Yang et al., 2019), as shown in **Figure 1**.

In addition, under the normal operation and accident conditions of PWR, the key thermal-hydraulic parameters span a wide range. For example, the pressure ranges from 2 to 17 MPa, the mass flux ranges from several hundred to nearly 5,000 kg/m²s, and the corresponding equilibrium quality ranges from -0.2 to 0.5. Obviously, such a wide range of thermal-hydraulic parameters may cover different CHF regimes (Groeneveld et al., 2018).

At present, due to the complex nature of two-phase flow with heat transfer in the rod bundle channel, the method for rod bundle CHF prediction is mainly CHF empirical correlation. In the development of CHF correlation, there is no classification for DNB and DO regime CHF conditions while all the CHF experimental data are put together to develop the CHF correlation (Chai et al., 2003). Moreover, once the application scope and original object of CHF empirical correlation are exceeded, the prediction accuracy will be significantly reduced. In addition, since the CHF empirical correlation usually depends on the specific correction factors, it has great uncertainty when it is extended to the condition lacking of CHF experimental data (Weisman and Pei, 1983).

Although extensive research has been carried out on CHF mechanisms and obtained several representative CHF mechanistic models with relatively high prediction accuracy (Zhang and Hewitt, 2016; Liu et al., 2020b), these CHF mechanistic models are all developed for a specific flow regime and often only applicable to DNB or DO regime CHF prediction. Obviously, the CHF prediction ability is limited to the flow or CHF regime. As Zeigarnik (Zeigarnik, 1996) pointed out, there is no universal flow boiling CHF mechanistic model that can predict CHF in the regimes of high subcooled, low subcooled, and saturated. Because there are different flow regimes and heat transfer modes in such a wide span range, only the main process can be modeled.

At present, different comprehensive CHF mechanistic models have been developed for prediction of DNB and DO regime CHF in round tubes (Kataoka et al., 1997; Kodama and Kataoka, 2002; Liu et al., 2019). However, the void fraction or quality is often used as the classification criterion for different CHF regimes in most of these comprehensive CHF mechanistic models. The accuracy and reliability of the CHF classification criterion still need further study.

Due to the complex nature of CHF phenomenon, the challenges of experimental measurement technology, and the characteristics of wide parameter range across different CHF regimes, the coexistence of various CHF mechanistic models at this stage seems reasonable and unchangeable.

In order to accurately and continuously predict the DNB and DO regime CHF in rod bundle channel under the wide parameter range, a feasible method is to classify the CHF conditions into different regimes and then establish the corresponding CHF mechanistic model based on the specific CHF-regime visualization phenomenon and mechanism hypothesis. Finally, different regimes of the CHF mechanistic model are combined to

form the comprehensive CHF mechanistic model throughout the CHF-regime criterion.

In previous studies, the author has obtained the classification criterion for CHF conditions in the rod bundle channel with the dimensional analysis method (Liu et al., 2021a) and developed the DNB regime CHF mechanistic model of superheated liquid layer depletion under turbulence fluctuation bubbles (Liu et al., 2021b). In this study, a comprehensive CHF mechanistic model covering different regimes of CHF prediction will be established by using the existing research results and the mature DO regime CHF mechanistic model. The comprehensive CHF mechanistic model will be assessed by the 5 × 5 full-length rod bundle CHF experimental data independently obtained by the Nuclear Power Institute of China (NPIC), and the statistical evaluation and parametric trend analysis will be carried out by using statistical methods.

EXISTING ROD BUNDLE CHF RESEARCH RESULTS

Rod Bundle CHF-Regime Criterion

In order to correctly distinguish the rod bundle CHF regimes, a general dimensionless rod bundle CHF correlation is obtained based on the dimensional analysis method (Liu et al., 2021a). The real vapor quality, Katto number, and boiling length are introduced to establish the basic form of the dimensionless CHF correlation. According to the deep analysis of the distribution trend of typical CHF experimental data and the CHF characteristics of different CHF regimes, the CHF in rod bundle are separated into DO, DNB, and HP-DNB regimes. The dimensionless equations between the boundaries of each regime are established, and a clearly defined map of characteristic regimes of CHF in rod bundle is determined.

The equation of the dividing line between DO and DNB regimes is,

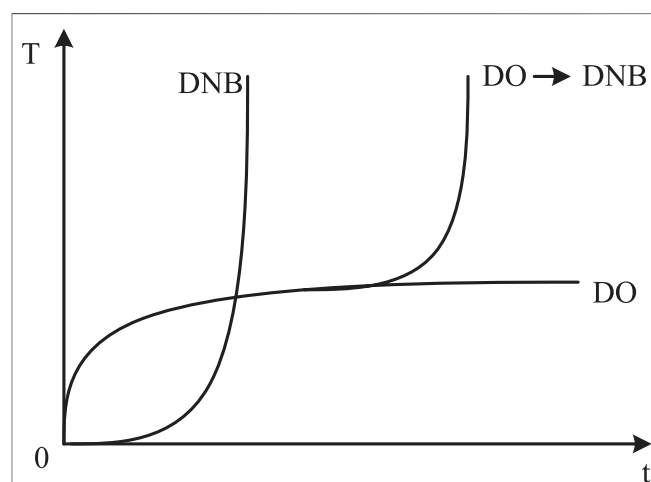


FIGURE 1 | Transition from DO to DNB regime CHF.

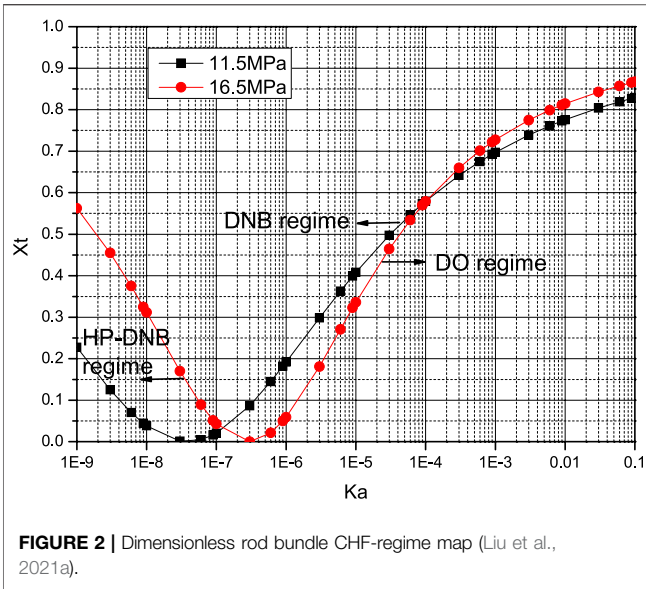


FIGURE 2 | Dimensionless rod bundle CHF-regime map (Liu et al., 2021a).

$$x_t = \left(\left(1.536 \ln \left(\frac{0.1}{(\rho_v/\rho_l)^{0.516} Ka^{0.055}} \right) \right)^2 / \right. \\ \left. \times \left(\left(1.536 \ln \left(\frac{0.1}{(\rho_v/\rho_l)^{0.516} Ka^{0.055}} \right) \right)^2 + 1 \right) \right),$$

where $Ka = \sigma \rho_l / G^2 l$.

The equation of the dividing line between DNB and HP-DNB regimes is,

$$x_t = \frac{\left(\ln \left(\frac{1.863 Ka^{0.06}}{(\rho_v/\rho_l)^{0.175}} \right) / (0.651 - 0.786 * (\rho_v/\rho_l)^{0.5}) \right)^2}{\left(\ln \left(\frac{1.863 Ka^{0.06}}{(\rho_v/\rho_l)^{0.175}} \right) / (0.651 - 0.786 * (\rho_v/\rho_l)^{0.5}) \right)^2 + 1}$$

Figure 2 shows the dimensionless rod bundle CHF-regime map for ρ_v/ρ_l of 0.1 (about 11.5 MPa) and 0.2 (about 16.5 MPa), respectively.

It can be seen from **Figure 2** that when the Katto number is large and real vapor quality is high, the CHF is corresponding to the DO regime. When the Katto number is small and real vapor quality is low, the CHF is corresponding to the DNB regime. The Katto number of the boundary point between DO and DNB regimes is about 10^{-7} . With the increase of pressure, the boundary point moves right, and the boundary line between DNB and HP-DNB regimes moves up. Consequently, the HP-DNB regime is expanded.

The above research results provide a theoretical basis for the classification of rod bundle CHF conditions.

DNB Regime CHF Mechanistic Model

Under subcooled and low quality flow boiling conditions, a general CHF mechanistic model is essential to the thermal-hydraulic design and safety analysis. Based on the mechanism

of superheated liquid layer depletion (Chun et al., 2000; Liu et al., 2021c), the net mass transfer from the bulk liquid to the superheated liquid layer caused by turbulent velocity fluctuations of flowing bubbles is determined, and a new calculation method of superheated liquid layer thickness is developed (Liu et al., 2021b). After matching with other constitutive equations, a novel CHF mechanistic model for subcooled and low quality flow boiling conditions has been developed, as shown in **Figure 3**.

For a fixed axial control volume Δz in the superheated liquid layer, the mass conservation equation is:

$$m - (m + \Delta m) - \Delta m_{\text{evap}} + m_{\text{turb}} = 0,$$

where Δm_{evap} is the mass flow rate of evaporation and m_{turb} is the turbulent mass flow rate transported from bulk flow to the superheated liquid layer.

After simplification,

$$\Delta m = v^* \rho \pi D \Delta z - \frac{(q - q_{\text{conv}}) \pi D \Delta z}{h_{fg}}$$

The radial net two-phase mass exchange rate from the bulk flow to the superheated liquid layer caused by turbulent velocity fluctuations (Liu et al., 2021b) is determined as

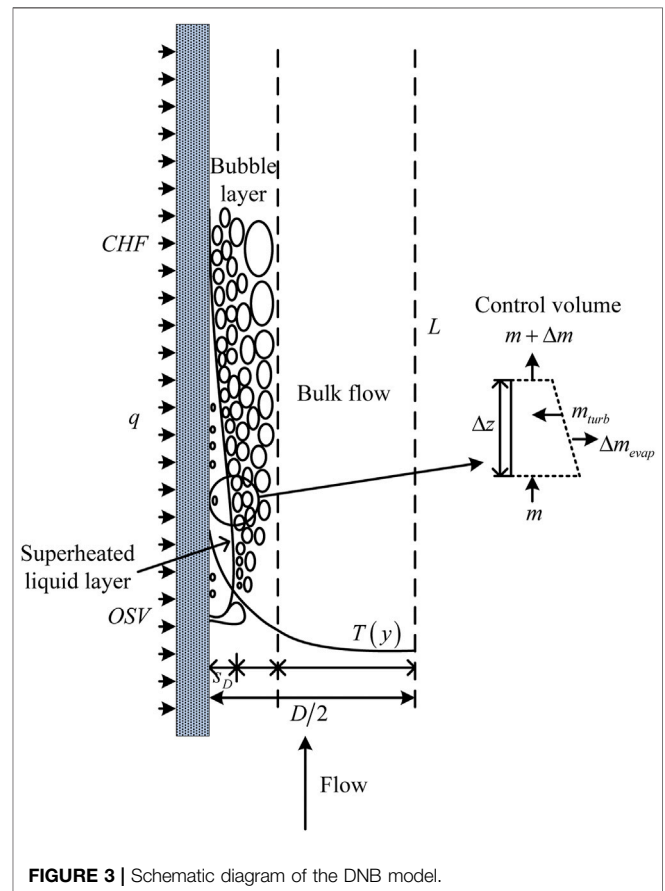
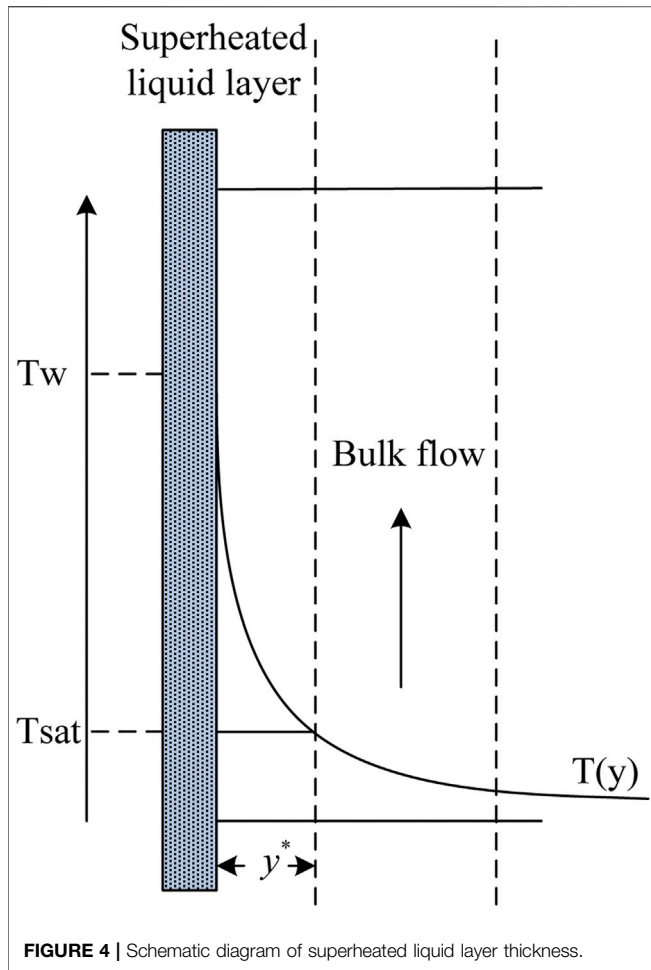


FIGURE 3 | Schematic diagram of the DNB model.



$$v^* = \sigma_v \left(\frac{1}{\sqrt{2\pi}} e^{-\frac{1}{2} \left(\frac{V_{11}}{\sigma_v} \right)^2} - \frac{1}{2} \left(\frac{V_{11}}{\sigma_v} \right) \operatorname{erfc} \left(\frac{1}{\sqrt{2}} \frac{V_{11}}{\sigma_v} \right) \right),$$

where σ_v is the standard deviation of velocity fluctuations. Then,

$$m_{\text{turb}} = v^* \rho \pi D \Delta z.$$

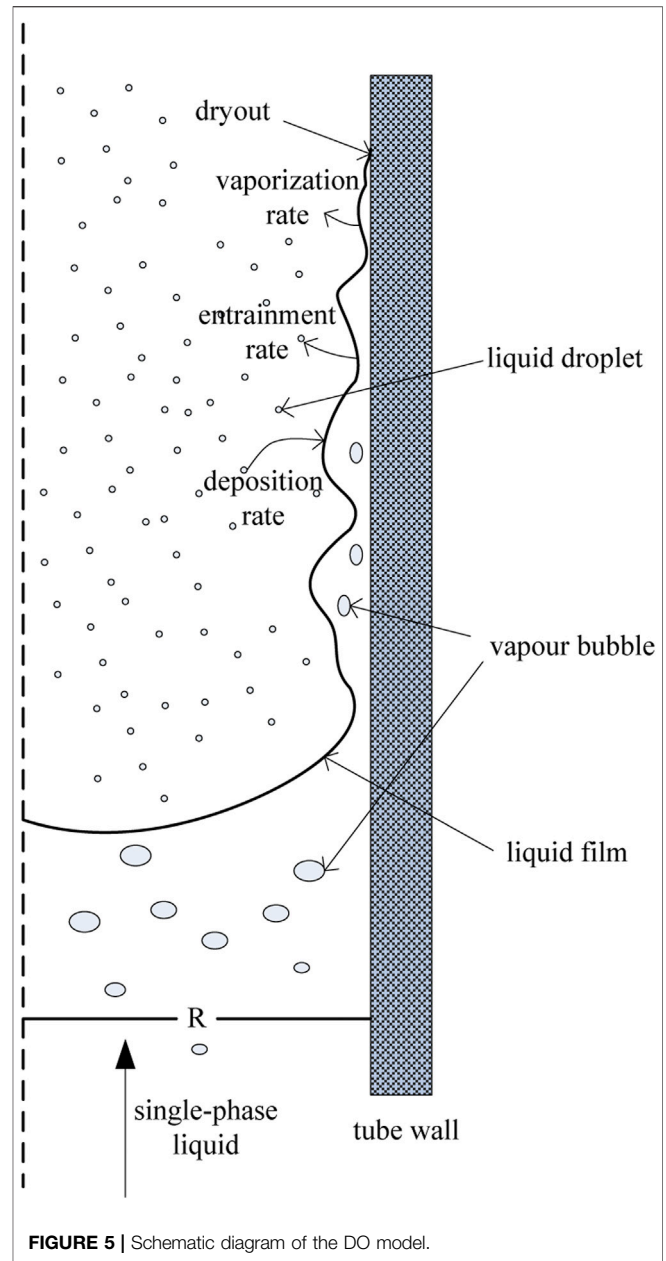
The calculation method of the superheated liquid layer thickness on the heating surface is proposed, as shown in **Figure 4**.

The superheated liquid layer thickness y^* is obtained directly through thermal equilibrium temperature distribution in the rod bundle channel.

$$T(y^+) = T_w - QPr y^+ \quad 0 \leq y^+ < 5,$$

$$T(y^+) = T_w - 5Q \left\{ Pr + 0.25 \ln \left[1 + Pr \left(\frac{y^+}{5} - 1 \right) \right] \right\} \quad 5 \leq y^+ < 30,$$

$$T(y^+) = T_w - 5Q \left[Pr + 0.25 \ln(1 + 5Pr) + \frac{1}{3} \ln \left(\frac{y^+}{30} \right) \right] \quad y^+ \geq 30,$$



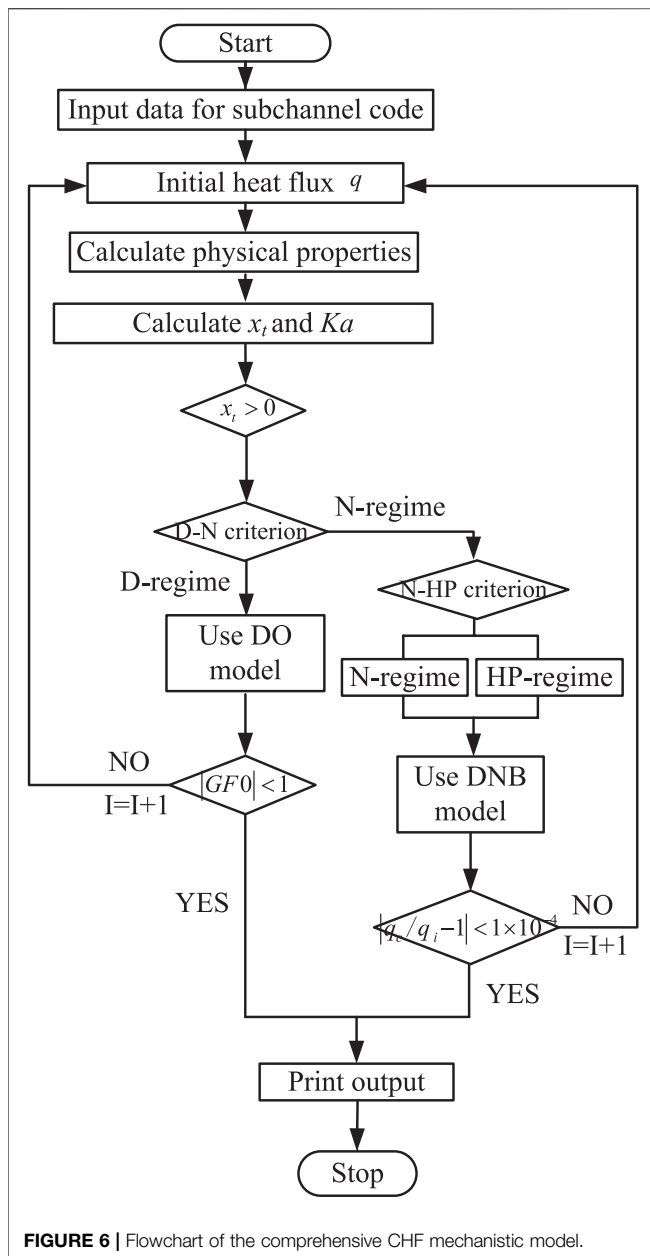
where T_w is the wall temperature, Pr is the Prandtl number of the liquid, and Q is a function of the local heat flux, liquid density, specific heat capacity, and friction velocity.

This DNB model is suitable for rod bundle CHF prediction under subcooled and low quality flow boiling conditions.

DO Regime CHF Mechanistic Model

In annular flow, the dryout of liquid film is determined by a balance between the liquid film evaporation, liquid droplet entrainment, and deposition from the entrained core (Groeneveld, 2013), as shown in **Figure 5**.

In the steady state, the mass conservation equation for the liquid film is:



$$\frac{D_e}{4} \frac{dG_f}{dz} = D - E - \frac{q}{h_{fg}}$$

Several models have been proposed for solution of the mass conservation equation. The models differ in the constitutive correlations representing the mechanisms of entrainment and deposition.

In this study, the DO regime CHF mechanistic model for BWR fuel assembly developed by Lim and Weisman (Lim and Weisman, 1988) is used (see reference Lim and Weisman (1988) for the subchannel division and solution steps of this model).

DEVELOPMENT OF COMPREHENSIVE CHF MECHANISTIC MODEL

In this section, the rod bundle CHF-regime criterion for DNB and DO regime CHF determined in *Rod Bundle CHF-Regime Criterion* is used to classify the CHF conditions. Then, the DNB regime CHF mechanistic model of superheated liquid layer depletion under turbulence fluctuation bubbles developed by the author is combined with the DO regime CHF mechanistic model of Lim and Weisman to form a comprehensive CHF mechanistic model covering the DNB and DO regime CHF prediction.

The detailed calculation process of the comprehensive CHF mechanistic model is shown in **Figure 6**.

First of all, input parameters such as pressure, mass flux, subcooling, and equivalent hydraulic diameter for subchannel code are needed to calculate local parameters in the current node. The initial heat flux is q and the corresponding physical properties x_t and Katto number are calculated.

For $x_t > 0$, the D-N criterion is used for judgment. If the current calculation condition belongs to DO regime, then the DO regime CHF model is used to calculate the liquid film flow rate. When the calculated liquid film flow rate is greater than the set value of $1 \text{ kg/m}^2\text{s}$, it means that CHF has not occurred in the current node, then the next node $I + 1$ is calculated. If the liquid film flow rate of the last node is still greater than the set value, it means that CHF will not occur in the whole subchannel, then the corresponding heat flux is evaluated.

If the current calculation condition belongs to the DNB regime, the N-HP criterion is used for judgment, and the DNB regime CHF model is used to calculate CHF. When the calculated CHF q_c does not meet the tolerance $|q_c/q_i - 1| < 1 \times 10^{-4}$, the next node $I + 1$ is calculated. If the last node still does not meet the tolerance, it means that CHF will not occur in the whole subchannel, then the corresponding heat flux is evaluated.

It should be noted that the comprehensive CHF mechanistic model established in this study can automatically and accurately judge and classify the current calculation conditions. Then, the appropriate CHF model is called to calculate and the corresponding CHF is printed. This comprehensive CHF model can accurately and continuously predict the DNB and DO regime CHF in rod bundle channel under the wide parameter range.

ASSESSMENT AND STATISTICAL EVALUATION

CHF Experimental Data

Aiming at the development of advanced Chinese fuel assemblies, NPIC has independently carried out the CHF experiment of 5×5 rod bundle with axial uniform and nonuniform heating, taking into account the geometry structure of rod bundle and flow subchannel, heating length, different grid arrangements, rod radial peaking factors, and the guide tube effects (Qin et al.,

TABLE 1 | CHF database and characteristics of each test.

Test series	Element geometry	Axial flux shape	Grid arrangement
TEST 1	Typical	Uniform	Half span
TEST 2	Typical	Uniform	Half span
TEST 5	Typical	Uniform	Half span
TEST 7	Guide tube	Uniform	Full span
TEST 8	Typical	Uniform	Full span
TEST 9	Typical	Cosine1.55	Full span

TABLE 2 | Parameter range of CHF experimental data.

Parameter	Range
Outlet pressure/MPa	2.1–16.7
Inlet mass flux/kg/m ² s	960–4760
Inlet temperature/°C	113–330
Local heat flux/kW/m ²	760–2611

2016). In this study, six CHF test series data are selected, and the database and its characteristics are shown in **Table 1**.

Table 2 shows the parameter range of CHF experimental data to assess the comprehensive CHF mechanistic model.

Calculation Method

The local thermal-hydraulic parameters in the 5 × 5 rod bundle of each CHF test series are calculated with the subchannel code CORTH (Liu et al., 2017), which was developed in NPIC for thermal-hydraulic analysis of reactor cores and experimental facilities with heating rod bundles. The rod bundle specific effects such as heating length, mixing strength, cold wall, and axial nonuniform heating are considered to account properly for the calculation of rod bundle local parameters (Dong et al., 2018; Liu et al., 2020a).

Figure 7 shows the subchannel numbering in a 5 × 5 rod bundle.

Assessment Results

Effect of Heating Length

First of all, the effects of heating length on CHF are validated by using the TEST 1, TEST 2, and TEST 5 experimental data. The distribution of P/M in these three series is shown in **Figure 8**.

It can be seen that the comprehensive CHF mechanistic model developed in this study can accurately and continuously predict the DNB and DO regime CHF in the rod bundle channel. All the P/M predicted by the comprehensive CHF mechanistic model are uniformly distributed in the vicinity of one within the mean error of ±22%.

Effect of Mixing Strength

The TEST 8 experimental data are used to validate the effect of spacer span (with intermediate mixing spacer grids to enhance the mixing strength) on CHF prediction. The distribution of P/M in this series is shown in **Figure 9**.

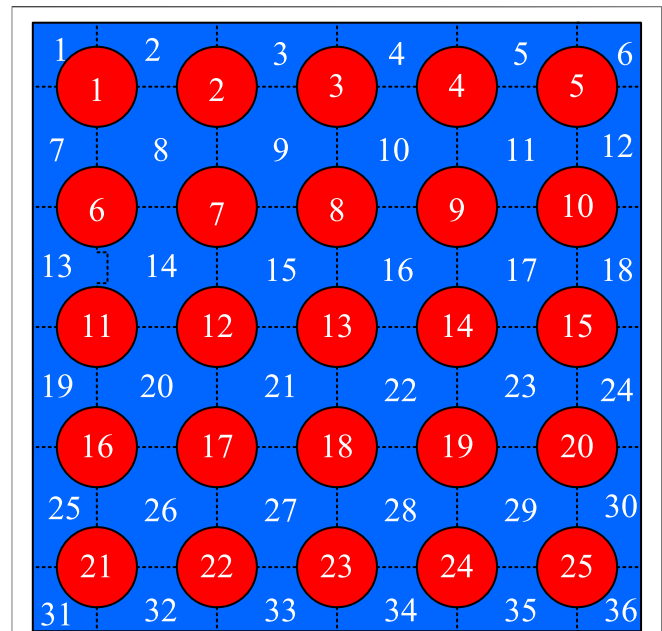


FIGURE 7 | Subchannel numbering in a 5 × 5 rod bundle.

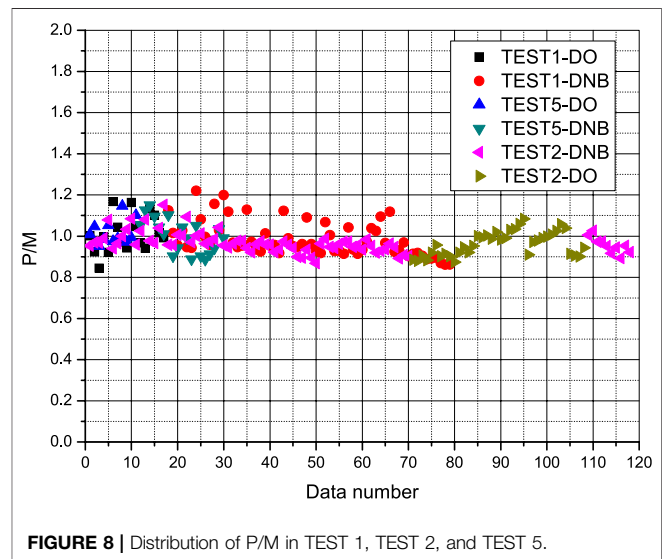


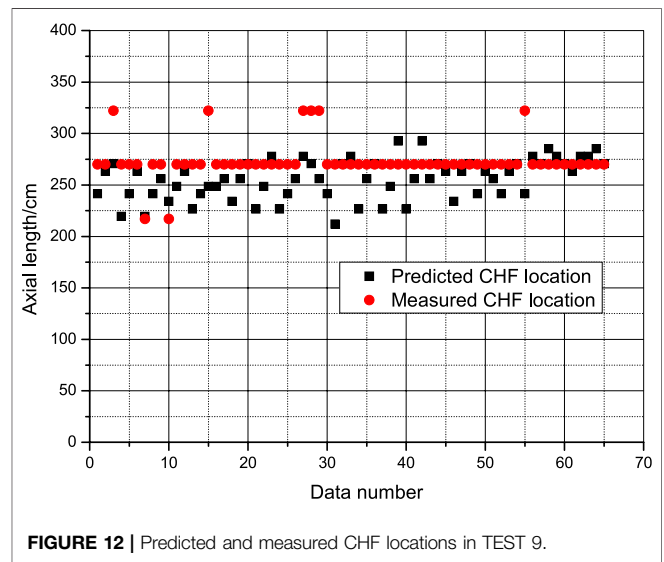
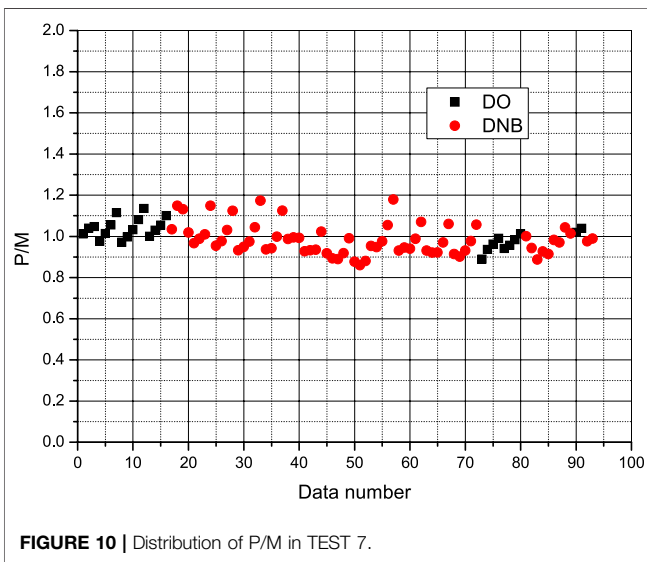
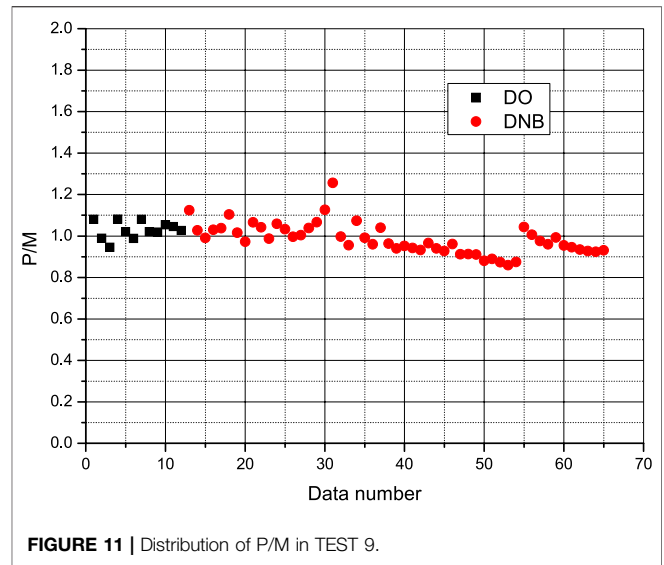
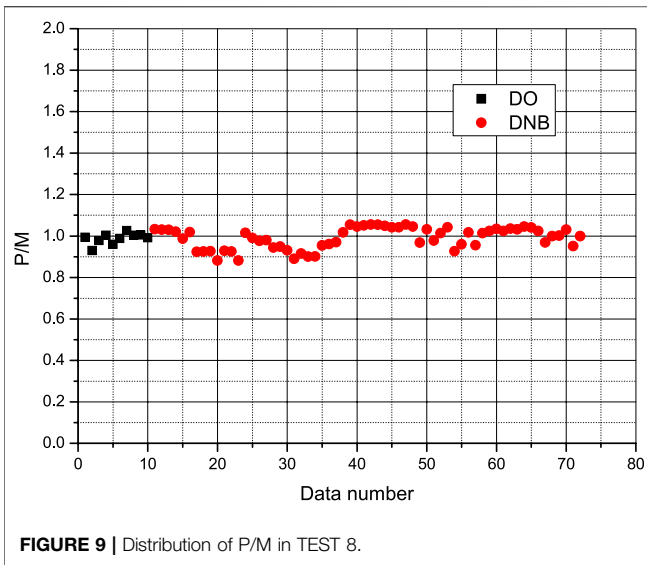
FIGURE 8 | Distribution of P/M in TEST 1, TEST 2, and TEST 5.

Similarly, all the P/M predicted by the comprehensive CHF mechanistic model are uniformly distributed near one within the mean error of ±12%.

Effect of Cold Wall

The effect of cold wall is validated by TEST 7 experimental data. The distribution of P/M in this series is shown in **Figure 10**.

It can be seen that all the P/M predicted by the comprehensive CHF mechanistic model are uniformly distributed near one within the mean error of ±18%.



Effect of Axial Nonuniform Heating

The TEST 9 experimental data are used to validate the effect of axial nonuniform heating. The distribution of P/M in this series is shown in **Figure 11**.

It can be seen that for the axial nonuniform heating CHF prediction, only one prediction comes up with mean error larger than 20%, and rest of the P/M are uniformly distributed near one within the mean error of $\pm 13\%$.

For the axial nonuniform heating of TEST 9, the CHF may not occur at the channel exit. **Figure 12** shows the comparison of the CHF mechanistic model–predicted locations with experimentally measured locations. It can be seen that the predicted CHF location is in good agreement with the experimentally measured location, and the deviation of some data points is only within one spacer span. This indicates that the comprehensive CHF mechanistic model can be used to predict the CHF location for the axial nonuniform heating condition.

Statistical Evaluation

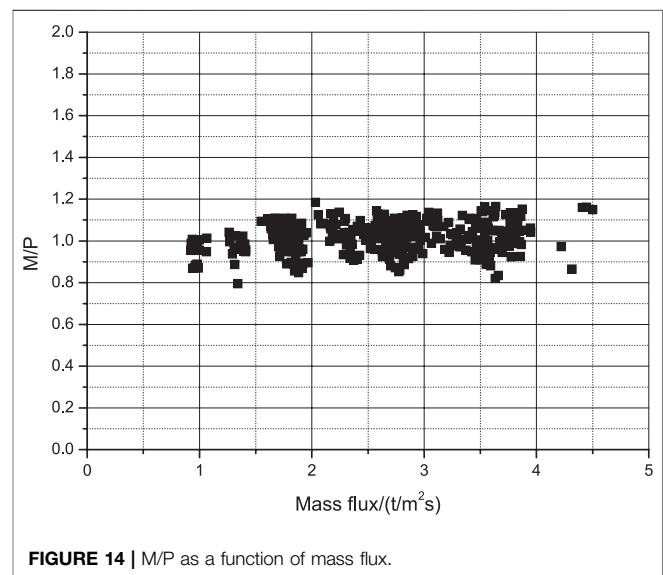
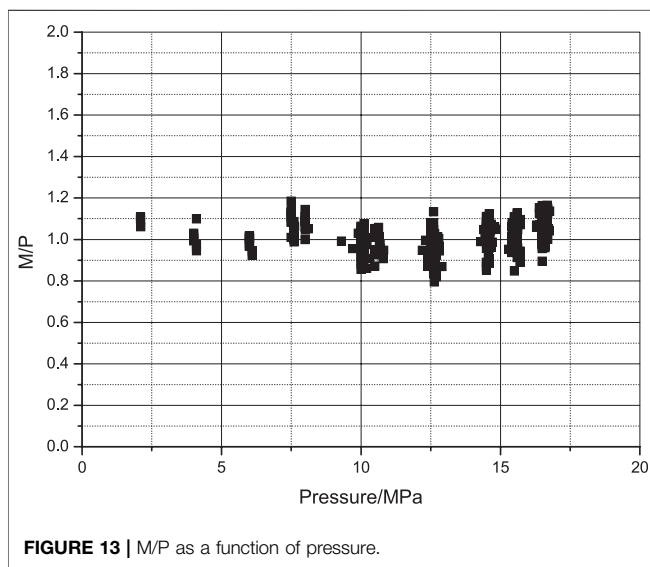
Table 3 shows the mean and standard deviation of M/P predicted by the CHF mechanistic model and CF-DRW correlation (Liu W. et al., 2020) based on the CHF experimental data shown in *CHF Experimental Data*. It can be seen that the mean and standard deviation of M/P with these two prediction methods are quite identical.

Figures 13–15 show the distributions of M/P as a function of independent variables such as local pressure, mass flux, and quality, respectively. It can be seen that the distribution of M/P with local pressure, mass flux, and quality have no obvious systematic bias.

Figure 16 shows the flux predicted by the CHF mechanistic model, P, as a function of experimental measured flux M. It can be seen that the distribution of heat fluxes calculated with the comprehensive CHF mechanistic model is well distributed along the 45 line

TABLE 3 | Statistical results of the CHF mechanistic model and CF-DRW correlation.

Test series	M/P	CF-DRW correlation	CHF mechanistic model
TEST 1	Mean	0.949	1.019
	Standard deviation	0.068	0.083
TEST 2	Mean	1.033	1.038
	Standard deviation	0.073	0.054
TEST 5	Mean	0.996	0.996
	Standard deviation	0.048	0.075
TEST 7	Mean	0.994	1.013
	Standard deviation	0.058	0.070
TEST 8	Mean	0.983	1.012
	Standard deviation	0.090	0.051
TEST 9	Mean	1.002	1.011
	Standard deviation	0.051	0.070
All	Mean	0.999	1.019
	Standard deviation	0.064	0.067



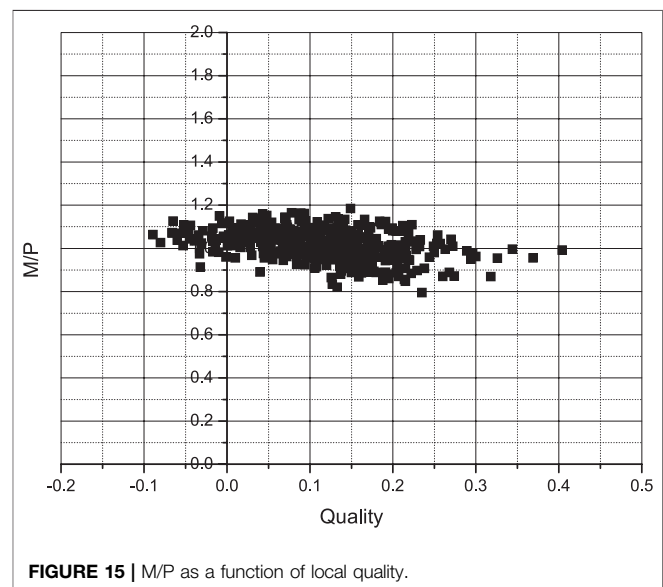
with measured CHF, and more than 95% experimental data are within the mean error of $\pm 15\%$.

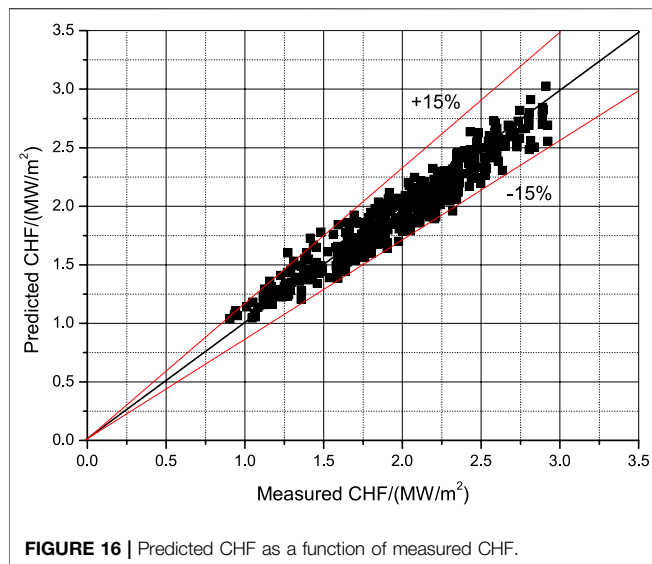
According to the statistical evaluation results, the comprehensive CHF mechanistic model is a promising candidate for rod bundle CHF prediction under the wide parameter range.

CONCLUSION

In this study, a comprehensive CHF mechanistic model covering DNB and DO regime CHF in a wide parameter range for the rod bundle channel is developed. This model is validated and statistically evaluated as a general CHF prediction method using the 5×5 rod bundle CHF experimental data. The important conclusions are as follows:

- (1) The comprehensive CHF mechanistic model developed in this study covers the parameter range of PWR under





normal operation and accident conditions and can accurately and continuously predict the DNB and DO regime CHF in the rod bundle channel.

- (2) The mean and standard deviation of all M/P are 1.019 and 0.067, which are identical to the prediction accuracy of CF-DRW correlation. No specific correction factors such as heating length, cold wall, and axial nonuniform heating effect are needed anymore.

REFERENCES

- Chai, G. H., Wang, X. H., Chen, Z. L., and Tao, S. S. (2003). Review of Correlation FC-2000 for Critical Heat Flux Calculation. *Nucl. Power Eng.* S2 (6), 84–87.
- Chun, T. H., Baek, W. P., and Chang, S. H. (2000). An Integral Equation Model for Critical Heat Flux at Subcooled and Low Quality Flow Boiling. *Nucl. Eng. Des.* 199, 13–29. doi:10.1016/s0029-5493(00)00224-7
- Dong, S., Liu, W., Liu, Y., et al. (2018). Application of the Improved Spacer Grid Model in Subchannel Analysis Code. *Nucl. Technol.* 205 (1-2), 352–363. doi:10.1080/00295450.2018.1491182
- Groeneveld, D. (2013). “The Critical Heat Flux Story,” in The 15th International Topical Meeting on Nuclear Reactor Thermal Hydraulics, Pisa, Italy, May 12–17.
- Groeneveld, D. C., Ireland, A., Kaizer, J., and Vasic, A. (2018). An Overview of Measurements, Data Compilations and Prediction Methods for the Critical Heat Flux in Water-Cooled Tubes. *Nucl. Eng. Des.* 331, 211–221. doi:10.1016/j.nucengdes.2018.02.031
- Kataoka, I., Kodama, S., Tomiyama, A., and Serizawa, A. (1997). Study on Analytical Prediction of Forced Convective CHF Based on Multi-Fluid Model. *Nucl. Eng. Des.* 175, 107–117. doi:10.1016/s0029-5493(97)00167-2
- Kodama, S., and Kataoka, I. (2002). “Study on Analytical Prediction of Forced Convective chf in the Wide Range of Quality,” in 10TH International Conference on Nuclear Engineering, Arlington, VA, USA, April 14–18.
- Lim, J. C., and Weisman, J. (1988). A Phenomenologically Based Prediction of Rod-Bundle Dryout. *Nucl. Eng. Des.* 105 (3), 363–371. doi:10.1016/0029-5493(88)90256-7
- Liu, W., Peng, S., Jiang, G., and Liu, Y. (2021a). Analytical Investigation on Rod Bundle CHF-Regime Criterion Based on Dimensionless Groups. *Int. J. Therm. Sci.* 159, 106571. doi:10.1016/j.ijthermalsci.2020.106571
- Liu, W., Peng, S., Jiang, G., and Liu, Y. (2021b). Development and Assessment of a New CHF Mechanistic Model for Subcooled and Low Quality Flow Boiling. *Int.*

- (3) The local pressure, mass flux, and quality do not have any effects on the average deviations of the predicted flux P from the measured flux M . This shows that the comprehensive CHF mechanistic model is a promising candidate for rod bundle CHF prediction under the wide parameter range.

DATA AVAILABILITY STATEMENT

The original contributions presented in the study are included in the article/Supplementary Material; further inquiries can be directed to the corresponding author.

AUTHOR CONTRIBUTIONS

WL: Conceptualization, methodology, and writing—original draft preparation. SP: Supervision. GJ: Data curation and validation. YL: Software and writing—reviewing and editing. All authors read and contributed to the manuscript.

FUNDING

The authors express their appreciation to the Nuclear Power Institute of China for their financial support.

- J. Heat Mass Transfer* 165, 120641. doi:10.1016/j.ijheatmasstransfer.2020.120641
- Liu, W., Peng, S., Jiang, G., Liu, Y., Du, S., Zhang, Y., et al. (2020). Development and Assessment of a New Rod-Bundle CHF Correlation for China Fuel Assemblies. *Ann. Nucl. Energy* 138, 107175. doi:10.1016/j.anucene.2019.107175
- Liu, W., Peng, S., Shan, J., Jiang, G., Liu, Y., Deng, J., et al. (2021c). Applicability Research of Round Tube CHF Mechanistic Model in Rod Bundle Channel. *Nucl. Eng. Technol.* 53, 439–445. doi:10.1016/j.net.2020.07.023
- Liu, W., Shan, J., Peng, S., Jiang, G., and Liu, Y. (2019). The Study of Critical Heat Flux in Upflow Boiling Vertical Round Tube under High Pressure. *Sci. Technol. Nucl. Installations* 2019, 1–14. doi:10.1155/2019/3695685
- Liu, Y., Dong, S., Shan, J., Zhang, B., Jiang, L., Liu, W., et al. (2020a). A Phenomenological CHF Model for Mixing-Vane Spacers in a Subchannel of a Rod Bundle. *Ann. Nucl. Energy* 142, 107445. doi:10.1016/j.anucene.2020.107445
- Liu, Y., Liu, W., Shan, J., Zhang, B., and Leung, L. K. H. (2020b). A Mechanistic Bubble Crowding Model for Predicting Critical Heat Flux in Subchannels of a Bundle. *Ann. Nucl. Energy* 137, 107085. doi:10.1016/j.anucene.2019.107085
- Liu, Y., Tan, C., Pan, J., et al. (2017). Development of Self-Reliant Subchannel Analysis Code CORTH. *Nucl. Power Eng.* 38 (6), 158–162.
- Qin, S., Lang, X., Xie, S., Li, P., Zhuo, W., Liu, W., et al. (2016). Experimental Investigation on Repeatability of CHF in Rod Bundle with Non-uniform Axial Heat Flux Distribution. *Prog. Nucl. Energy* 90, 151–154. doi:10.1016/j.pnucene.2016.03.015
- Qu, W., Xiong, J., Chen, S., and Cheng, X. (2019). High-fidelity PIV Measurement of Cross Flow in 5×5 Rod Bundle with Mixing Vane Grids. *Nucl. Eng. Des.* 344, 131–143. doi:10.1016/j.nucengdes.2019.01.021
- Tong, L. S. (1967). Heat Transfer in Water-Cooled Nuclear Reactors. *Nucl. Eng. Des.* 6 (4), 301–324. doi:10.1016/0029-5493(67)90111-2

- Weisman, J., and Pei, B. S. (1983). Prediction of Critical Heat Flux in Flow Boiling at Low Qualities. *Int. J. Heat Mass Transfer* 26 (10), 1463–1477. doi:10.1016/s0017-9310(83)80047-7
- Xiong, J., Qu, W., Zhang, T., Chai, X., Liu, X., and Yang, Y. (2020). Experimental Investigation on Split-Mixing-Vane Forced Mixing in Pressurized Water Reactor Fuel Assembly. *Ann. Nucl. Energ.* 143, 107450. doi:10.1016/j.anucene.2020.107450
- Yang, B.-W., Han, B., Liu, A., and Wang, S. (2019). Recent Challenges in Subchannel Thermal-Hydraulics-CFD Modeling, Subchannel Analysis, CHF Experiments, and CHF Prediction. *Nucl. Eng. Des.* 354, 110236. doi:10.1016/j.nucengdes.2019.110236
- Zeigarnik, Y. A. (1996). Universal Model of Critical Heat Flux of Subcooled Liquid Boiling in Channels. *High temperature* 34 (1), 48–52.
- Zhang, H., and Hewitt, G. F. (2016). New Models of Droplet Deposition and Entrainment for Prediction of CHF in Cylindrical Rod Bundles. *Nucl. Eng. Des.* 305, 73–80. doi:10.1016/j.nucengdes.2016.04.044

Conflict of Interest: The authors declare that the research was conducted in the absence of any commercial or financial relationships that could be construed as a potential conflict of interest.

Copyright © 2021 Liu, Peng, Jiang and Liu. This is an open-access article distributed under the terms of the Creative Commons Attribution License (CC BY). The use, distribution or reproduction in other forums is permitted, provided the original author(s) and the copyright owner(s) are credited and that the original publication in this journal is cited, in accordance with accepted academic practice. No use, distribution or reproduction is permitted which does not comply with these terms.

NOMENCLATURE

D channel diameter (m)/droplet deposition rate ($\text{kg}/\text{m}^2\text{s}$)

De equivalent diameter (m)

E entrainment rate ($\text{kg}/\text{m}^2\text{s}$)

G mass flux ($\text{kg}/\text{m}^2\text{s}$)

h_{fg} latent heat of vaporization (kJ/kg)

Ka Katto number

m mass flow rate (kg/s)

M measured CHF (MW/m^2)

p pressure (MPa)

P predicted CHF (MW/m^2)

Pr Prandtl number

q heat flux (MW/m^2)

q_c critical heat flux (MW/m^2)

T temperature ($^{\circ}\text{C}$)

v' radial velocity (m/s)

v^{*} net mass exchange rate (m/s)

V_{II} vapor generation rate (m/s)

x equilibrium quality

x_t real vapor quality

y^{*} distance from the wall (m)

z axial coordinate (m)

ρ density (kg/m^3)

SUBSCRIPTS

conv forced convection

evap evaporation

l liquid

turb turbulence fluctuations

v vapor

w wall

sat saturation condition